PROCEEDINGS OF SPIE

SPIEDigitalLibrary.org/conference-proceedings-of-spie

New approach for luminescence sensing based on machine learning

Francesca Venturini, Michael Baumgartner, Umberto Michelucci

Francesca Venturini, Michael Baumgartner, Umberto Michelucci, "New approach for luminescence sensing based on machine learning ," Proc. SPIE 10937, Optical Data Science II, 109370H (1 March 2019); doi: 10.1117/12.2508969

SPIE.

Event: SPIE OPTO, 2019, San Francisco, California, United States

New approach for luminescence sensing based on machine learning

Francesca Venturini[a,b], Michael Baumgartner[a], and Umberto Michelucci[b]

[a]Institute of Applied Mathematics and Physics, Zurich University of Applied Sciences, Technikumstrasse 9, 8401 Winterthur, Switzerland
[b]TOELT LLC; Birchlenstrasse 25, 8600 Dbendorf, Switzerland

ABSTRACT

Luminescence sensors are based on the determination of emitted intensity or decay time when a luminophore is in contact with its environment. Changes of the environment, like temperature or analyte concentration cause a change in the intensity and decay rate of the emission. Typically, since the absolute values of the measured quantities depend on the specific sensing element and scheme used, a sensor needs an analytical model to describe the dependence of the quantity to be determined, for example the oxygen concentration concentration, from sensed quantity, for example the decay time. Additionally, since the details of this dependence are device specific, a sensor needs to be calibrated at known reference conditions. This work explores an entirely new artificial intelligence approach and demonstrates the feasibility of oxygen sensing through machine learning. The new developed neural network is used for optical oxygen sensing based on luminescence quenching. After training the neural network on synthetic data, it was tested on measured data to verify the prediction of the model. The results show a mean deviation of the predicted from the measured concentration of 0.5 % air, which is comparable to many commercial and low-cost sensors. The accuracy of the model predictions is limited by the ability of the generated data to describe the measured data, opening up future possibilities for significant improvement by performing the training on experimental data. In this work the approach is tested at different temperatures, showing its applicability in the entire range relevant for biological applications. This work demonstrates the applicability of this new approach based on machine learning for the development of a new generation of optical luminescence oxygen sensors without the need of an analytical model of the sensing element and sensing scheme.

Keywords: artificial intelligence; neural network; machine learning; oxygen sensor; luminescence; optical sensor; luminescence quenching; phase fluorimetry

1. INTRODUCTION

The measurement of oxygen concentration is of great interest in many fields ranging from biomedical imaging, environmental monitoring, process control, and chemical industry, to mention only a few. Among the different optical methods, the quenching of luminescence by the oxygen molecules is an established method both for laboratory and for industrial sensors.[1,2]

A dye molecule, called in this work indicator, is embedded in a matrix permeable to oxygen. Its luminescence is quenched due to the dynamical collisions with molecular oxygen. This process leads to a reduction by an amount which depends on the oxygen concentration of both the intensity and decay time of the luminescence.[3–5] The luminescence quenching measurement principle has been succesfully commercialized since several years and has replaced other oxygen sensing technologies.[6]

Sensors based on luminescence quenching are based on an empirical and often only approximate multi-parametric model to capture the dependence of the sensing quantity (e.g., intensity or decay time) on influencing factors. These include, for example, the temperature, which strongly influences both the luminescence and the quenching mechanism, the quenching rate constant of the indicator, or the solubility of oxygen in the matrix which serves as a solvent for it. The resulting analytical model is therefore highly specific of the system used.[7–10] This specificity and variations due to hardware-related tolerances are usually accounted for by a device-specific

Send correspondence to F. Venturini: francesca.venturini@zhaw.ch

Optical Data Science II, edited by Bahram Jalali, Ken-ichi Kitayama, Proc. of SPIE Vol. 10937, 109370H · © 2019 SPIE · CCC code: 0277-786X/19/$18 · doi: 10.1117/12.2508969

calibration. Therefore, the complexity of the model, the lengthy calibration, and the potential changes during the application in the field, possibly neglected in the model, make an alternative approach highly interesting.

This work explores a new machine learning approach based on the development of a neural network model which learns to relate the sensed quantities to an oxygen concentration value. To the best of the author's knowledge, machine learning was never applied to phase-fluorimetry based luminescence sensing, only to time-resolved luminescence data.[11] Due to the lack of enough experimental data the training was performed with an artificially-created training dataset. The results show that the current network already achieves results comparable with many high-concentration commercial and compact sensors based on classical approaches.[6,12] In this work the robustness of the approach at different temperatures was investigated to test the feasibility for field applications. Potential for improvement is also identified, showing how this approach may allow a new generation of sensors.

2. MODEL FOR OXYGEN SENSING VIA LUMINESCENCE QUENCHING

The measurement of the oxygen concentration is performed thanks to the change of the luminescence intensity and decay time of a specific indicator in presence of O_2. The collision of the indicator with molecular oxygen act as a radiationless deactivation process resulting in a quenching of the luminescence. In the case of homogeneous media characterized by an intensity decay which is a single exponential, the decrease in intensity and lifetime are both described by the Stern-Volmer (SV) equation[3,4]

$$\frac{I_0}{I} = \frac{\tau_0}{\tau} = 1 + K_{SV} \cdot [O_2] \tag{1}$$

where I_0 and I, respectively, are the luminescence intensities in the absence and presence of oxygen, τ_0 and τ the decay times in the absence and presence of oxygen, K_{SV} the Stern-Volmer constant and $[O_2]$ indicates the oxygen concentration.

In many cases when the indicator is embedded in a substrate, the SV curve does not display a linear behavior as in equation (1).[1] Possible reasons may be, for example, heterogeneities of the micro-environment of the luminescent indicator, or the presence of static quenching. To describe this behavior a common model is the multi-site, or for two sites the two-site model,[13] in which the the SV curve is the sum of at least two contributions, characterized by different quanching rates, and written as

$$\frac{I_0}{I} = \left(\frac{f_1}{1 + K_{SV1} \cdot [O_2]} + \frac{f_2}{1 + K_{SV2} \cdot [O_2]} \right)^{-1} \tag{2}$$

where I_0 and I, respectively, are the luminescence intensities in the absence and presence of oxygen, f_1 and $f_2 = 1 - f_1$ are the fractions of the total emission for each component under unquenched conditions, K_{SV1} and K_{SV2} are the associated Stern-Volmer constants for each component, and $[O_2]$ indicates the oxygen concentration. Since $f_1 + f_2 = 1$, the following notation will be used in this work: $f_1 = f$ and $f_2 = 1 - f$. Although this model was introduced for luminescence intensities, it is frequently also used to describe the oxygen dependence of the decay times.

The measurement of the luminescence decay time can be conveniently and cost-effectively realized in the frequency domain by modulating the the intensity of the excitation. In this method, also known as phase fluorimetry, the emitted luminescence light is also modulated but shows a phase shift θ due to the finite lifetime of the excited state. For a single-exponential decay, the relation between these quantities is

$$\tan \theta = \omega \, \tau \tag{3}$$

where ω is the angular frequency and τ is the luminescence decay time. For a multi-exponential intensity decay, is not meaningful to define a single decay time and the relationship between phase shift and decay times must be calculated through the sine and cosine transforms of the intensity decay.[4,14–17] However, to overcome the eccesive complexity of an implementation, it is typical to introduce an apparent decay time and to relate it to the oxygen concentration as

$$\frac{\tan \theta_0}{\tan \theta} = \left(\frac{f}{1 + K_{SV1} \cdot [O_2]} + \frac{1 - f}{1 + K_{SV2} \cdot [O_2]} \right)^{-1} \tag{4}$$

where θ_0 and θ, respectively, are the phase shifts in the absence and presence of oxygen, f and $1-f$ are the fractions of the total emission for each component under unquenched conditions, K_{SV1} and K_{SV2} are the associated SV constants for each component, and $[O_2]$ indicates the oxygen concentration. The quantities f, K_{SV1}, and K_{SV2} may result frequency dependent, an artifact of the approximation of the model. The equation (4), although only an approximation, was used in this work to generate the synthetic data for the training due to its simplicity.

3. EXPERIMENTAL SETUP

The sample used for the characterization and test was a commercially available Pt-TFPP-based oxygen sensor spot (PSt3, PreSens Precision Sensing GmbH, Regensburg, Germany). To control the temperature of the samples, these were placed in good thermal contact with a copper plate, placed in a thermally insulated chamber. The temperature of this plate was adjusted at a fixed value between 0 °C and 45 °C using a Peltier element and stabilized with a temperature controller (PTC10, Stanford Research Systems, Sunnyvale, CA USA). The thermally insulated chamber was connected to a self-made gas-mixing apparatus which enabled to vary the oxygen concentration between 0 % and 20 % vol O_2 by mixing nitrogen and dry air. In the following, the concentration of oxygen will be given in % of the oxygen concentration of dry air and indicated with % air. This means, for example, that 20 % air corresponds to 4 % vol O_2 and 100 % air corresponds to 20 % vol O_2. The absolute error on the oxygen concentration adjusted with the gas-mixing apparatus is estimated to be below 1 % air.

The optical setup used in this work for the luminescence measurements is shown schematically in Fig. 1.

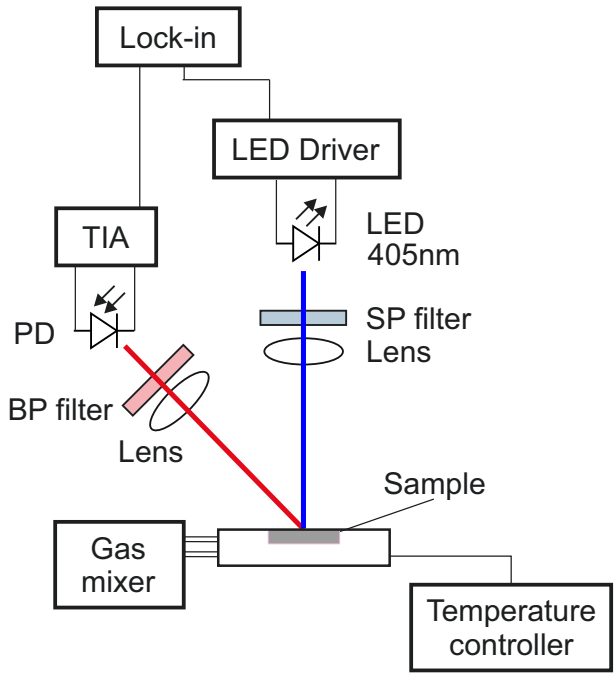

Figure 1. Scheme of the optical experimental setup. Blue is the excitation, red the luminescence optical path. PD: photodiode; SP filter: short pass filter; BP filter: band pass filter; TIA: trans-impedance amplifier.

The samples were excited with a 405 nm LED (VAOL-5EUV0T4, VCC Visual Communications Company), whose light was filtered by an OD5 short pass filter with cut-off at 498 nm (Semrock 498 SP Bright Line HC short pass) and focused on the surface of the samples with a collimation lens. The luminescence light was focused by a lens on a photodiode (SFH 213 Osram). The luminescence emission was filtered by a band pass filter composed of an OD5 long pass filter with cut-off at 594 nm (Semrock 594 LP Edge Basic long pass) and an OD5 short pass filter with cut-off at 682 nm (Semrock 682 SP Bright Line HC short pass) to suppress stray light and light reflected by the sample surface. Both the LED driver and the trans-impedance amplifier (TIA) are self-made.

For the frequency generation and the phase detection a two-phase lock-in amplifier (SR830, Stanford Research Inc.) was used. The modulation frequency was varied between 200 Hz and 20 kHz.

4. MACHINE LEARNING APPROACH

The machine learning approach of this work consist in using a tuned feed-forward neural network, which learns to relate an input measured quantity to an output quantity from a large number of examples, making the mathematical description of the luminescence decay irrelevant.[18] The method consists in taking a large number m of measurements of the ratio of equation (5)

$$r(\omega, T, [O_2]) \equiv \frac{\tan\theta(\omega, T, [O_2])}{\tan\theta(\omega, T, [O_2] = 0)} \tag{5}$$

at 16 known values of the modulation frequency and for a set of values of the oxygen concentration uniformly distributed in the range of interest, and use it to train a neural network. Since a large volume of data was not available, synthetic data were generated and used for the training of the network. The method and the study of the network architecture are described in detail in a previous work and will not repeated here.[19]

The steps of the method[19] are shown in the flowchart of Fig. 2. The steps are the following:

(i) Data acquisition for different values of frequency, temperature, and oxygen concentration.

(ii) Determination of a numerical approximation, via interpolation, of the quantities $KSV_1(\omega)$, $KSV_2(\omega)$, and $f(\omega)$ at the chosen temperature T_1.

(iii) Creation of the dataset S with m synthetic measurements using the numerical approximation.

(iv) Split of the dataset S into a training dataset S_{train} composed of 80 % of the observations, and a development S_{dev} dataset composed of 20 % of the observations.

(v) Training of several neural network models on the artificial training dataset S_{train}.

(vi) Check for a high-variance (or overfitting) using S_{train} and S_{dev} datasets.

(vii) Application of the trained neural network model to the experimental dataset to predict the oxygen concentration and comparison with the measured $[O_2]$ quantities.

For the analysis performed in this paper a network with 3 layers and 10 neurons in each layer has been used. Increasing the effective network complexity after a certain level does not improve the performance of the network because of the differences between experimental measured and synthetically generated data including the experimental error.[19] Therefore, in this work the network was not modified.

The metric used to check the model performance is the absolute error (AE). This is defined, as the absolute value of the difference between the predicted and the measured $[O_2]^{[j]}$ value for a given observation j corresponding to a given value of $[O_2]$

$$\mathrm{AE}^{[j]} = |[O_2]^{[j]}_{pred} - [O_2]^{[j]}_{meas}|. \tag{6}$$

A further metric calculated for a given temperature T is the mean absolute error (MAE) and calculated as

$$\mathrm{MAE}(S_{test}) = \frac{1}{|S_{test}|} \sum_{j \in S_{test}} |[O_2]^{[j]}_{pred} - [O_2]^{[j]}_{meas}|. \tag{7}$$

where with S_{test} indicates the dataset used for the validation of the neural network model. S_{test} contains the 10 experimental observations measured at a given temperature for the different values of the oxygen concentration $[O_2]$.

The neural network model have been developed with Python™, in particular with the packages *scipy*[20] and TensorFlow™.

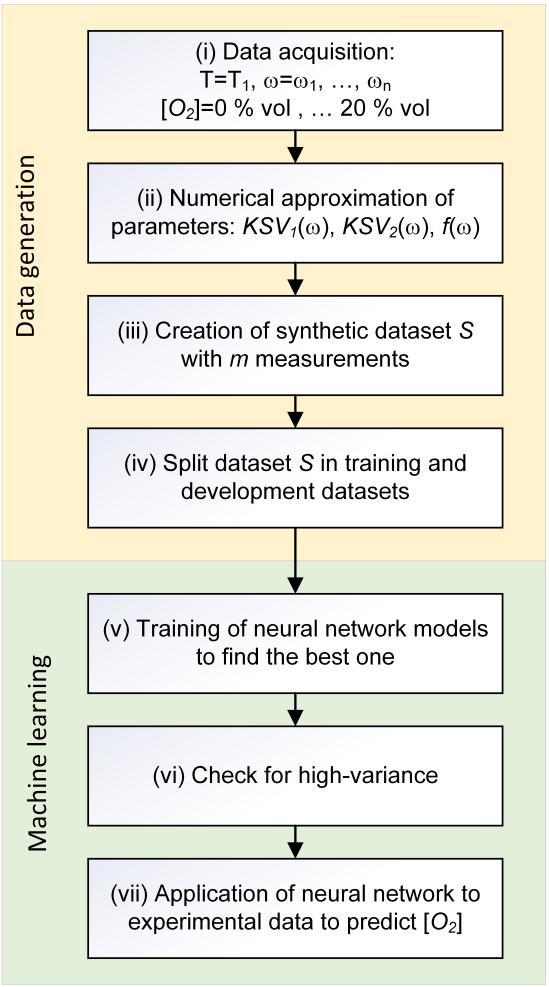

Figure 2. Schematic overview of the steps of the machine learning approach.[19]

5. RESULTS

Fig. 3 shows the dependence of the phase shift from the the oxygen concentration and temperature. Here the phase shifts measured at a fixed modulation frequency of 6 kHz are plotted as $\tan\theta_0/\tan\theta$ for three selected temperatures. The measurements in Fig. 3 show that, since the functional form of the $\tan\theta_0/\tan\theta$ is the same for all temperatures, the artificial intelligence approach is expected to work similarly well for all the temperatures in the range studied. The performance of the neural network for the different temperatures measured, evaluated as the absolute error defined in equation (6) is shown inf Fig. 4. For each temperature the absolute error is calculated for the available oxygen concentrations and displayed as a box plot, where the median is visible as a red line.

The results of Fig. 4 show that the machine learning approach works very well for all the temperatures, predicting the oxygen concentrations below 100 % air with an absolute error below 1 % air and a median absolute error of the order of 0.5 % air. The prediction of the concentration corresponding to 100 % air is shown in Fig. 4 as a separate dot because characterized by a higher absolute error, around 2 % air, little dependent on the temperature.

The distribution of the absolute error with the oxygen concentration at a single temperature is shown as example for 25 °C in 5. From the figure is clearly visible that the AE, which is below 0.5 % air for lower oxygen concentrations, increases for $[O_2]$ above30 % air. Again, the AE reaches the highest concentration at 100 % air.

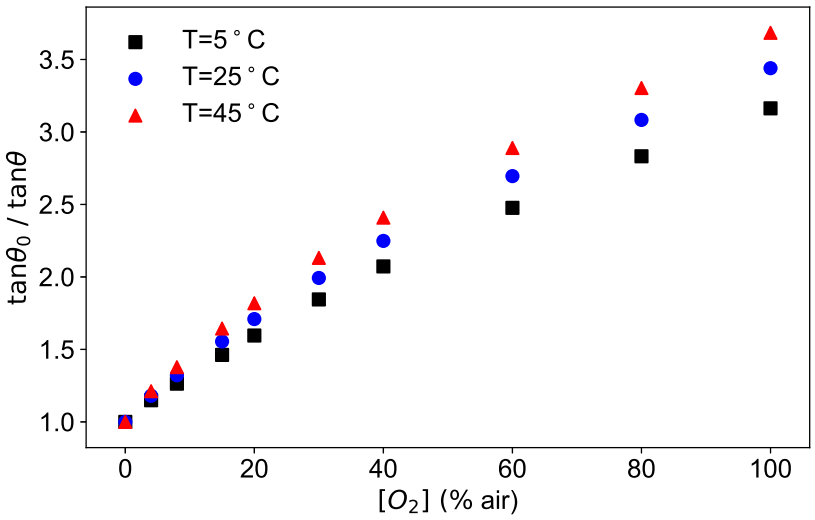

Figure 3. Phase shift measured for a modulation frequency of 6 kHz at the temperatures 5 °C, 25 °C, and 45 °C as a function of the oxygen concentration.

The origin of the strongest deviation for concentrations of 100 % air was investigated in detail and found to be due to the approximation of the conventional model describing the quenching of the luminescence of equation (4), which was used to generate the training data.[19] In other words, the training was performed with synthetic data which do not approximate well enough the experimental measurements. So the network learned from a dataset with slightly different functional shape than the experimental dataset. Thus, the absolute error could be reduced using experimental measures as a training dataset, allowing to achieve even better predictions of the oxygen concentration.

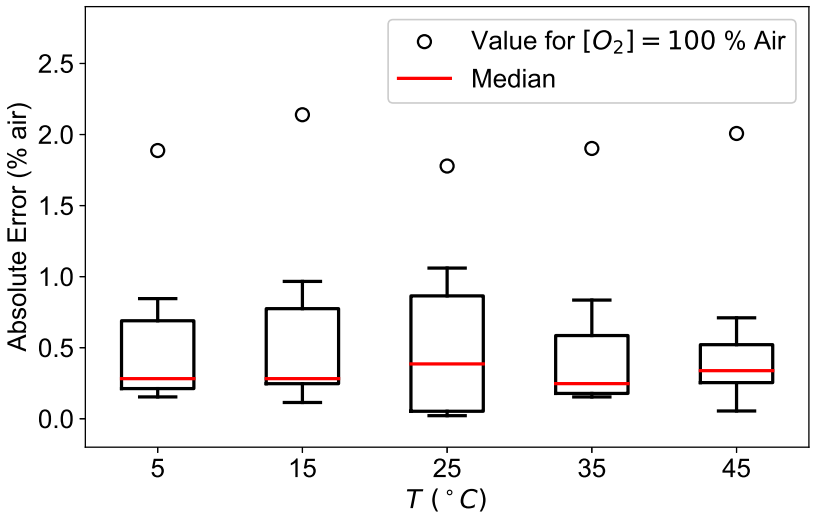

Figure 4. Performance of the neural network: absolute error distribution for different concentrations calculated at the temperatures of 5 °C, 15 °C, 25 °C, 35 °C, and 45 °C. The absolute error corresponding to 100 % air is shown separately as circle.

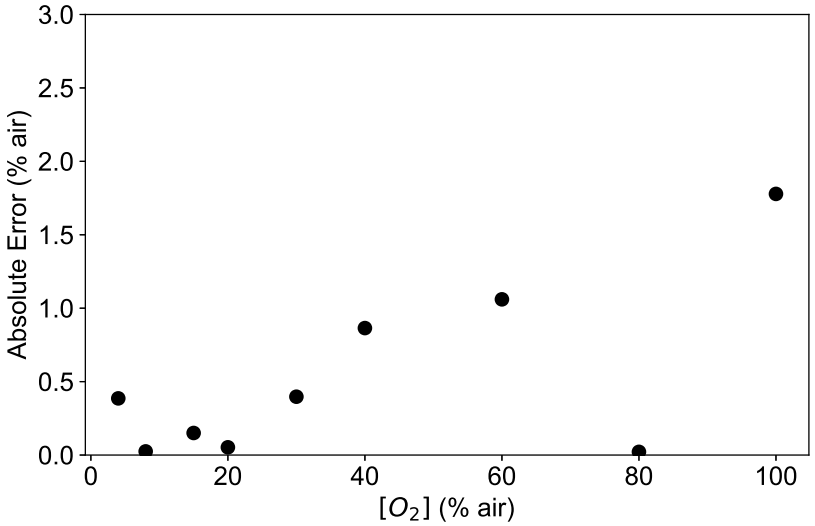

Figure 5. Absolute error of the neural network model prediction applied to the experimental data at the temperatures 25 °C.

6. CONCLUSIONS

This work investigates the applicability of a novel machine learning approach and demonstrates its relevancy for optical oxygen luminescence sensing. The optimized neural network learns to relate the measured quantity, the phase shift, to the oxygen concentration, without the need of an analytical model describing the quenching of luminescence and its dependence from the parameters of interest. The proposed artificial intelligence approach has therefore the advantage to be applicable even if the observed Stern-Volmer curves deviate from the common multi-parameter approximate models, which is the case with many commercial and low-cost sensors. The sensor-specific deviations, which may be caused, for example, by the sensing element and the immobilization of the indicators in the substrate, or even by sensor-specific hardware-related component, like absorption filters or glues, do not play any role in the described approach because they can be learned by the neural network.

The neural network is characterized by a feed-forward architecture, and learns effectively to predict the oxygen concentration with a median absolute error of 0.5 % air. The results show that the absolute error increases with higher concentrations, going from below 0.5 % air to a maximum of 2 % air at 100 % air. The main contribution to the absolute error was identified in the poor agreement of the conventional model describing the quenching of the luminescence, which was used to generate the training data. The performance of the network is expected to increase significantly by performing the training on experimental data, achieving an even better agreement of the prediction with the measurements. The analysis was carried out at different temperatures in the range between 5 °C and 45 °C, which is the range relevant for biophysical applications. The results show the approach works well for all the temperatures studied.

In conclusion, this work shows that, a feed-forward neural network is capable to capture the effects of the relevant influencing parameters studied in their entire range of application: modulation frequency, oxygen concentration and temperature. Once the sensor hardware is given, that is all the optical, electronic, mechanical and chemical components are assembled, a neural network can be trained to learn to predict one, or possibly more, quantities of interests, in this work the oxygen concentration. The new approach opens up new possibilities in sensor development because all the device-specific characteristics can be accounted for by the trained neural network.

REFERENCES

[1] Wang X.-D.; Wolfbeis O. S. Optical methods for sensing and imaging oxygen: materials, spectroscopies and applications. *Chem. Soc. Rev.* **2014**, *43*, 3666-3761.

[2] Narayanaswamy, R.; Wolfbeis, O.S. Eds. *Optical sensors: Industrial Environmental and Diagnostic Applications*, 1st ed; Vol. 1. Springer Science & Business Media, Berlin, Germany, 2004; pp. 28-30.

[3] Quaranta, M.; Sergey M.B.; Klimant I. Indicators for optical oxygen sensors. *Bioanalytical reviews* **2012**, *4*, 115-157.

[4] Lakowicz, J. R. *Principles of Fluorescence Spectroscopy*, 3rd ed.; Springer, Singapore, 2006.

[5] Demas, J.N.; DeGraff, B.A.; Coleman, P.B. Oxygen Sensors Based on Luminescence Quenching. *Anal. Chem.* **1999**, *71*, 793A-800A.

[6] Wolfbeis, O.S. Luminescent sensing and imaging of oxygen: Fierce competition to the Clark electrode. *BioEssays* **2015**, *37*, 921-928.

[7] Draxler, S.; Lippitsch, M.E.; Klimant, I.; Kraus, H.; Wolfbeis, O.S. Effects of polymer matrixes on the time-resolved luminescence of a ruthenium complex quenched by oxygen. *Journal of Physical Chemistry* **1995**, *99*, 3162-3167.

[8] Hartmann, P.; Trettnak, W. Effects of polymer matrices on calibration functions of luminescent oxygen sensors based on porphyrin ketone complexes. *Anal. Chem.* **1996**, *68*, 2615-2620.

[9] Dini, F.; Martinelli, E.; Paolesse, R.; Filippini, D.; DAmico, A.; Lundstrm, I.; Di Natale, C. Polymer matrices effects on the sensitivity and the selectivity of optical chemical sensors. *Sensors and Actuators B: Chemical* **2011**, *154*, 220-225.

[10] Badocco, D.; Mondin, A.; Pastore, P.; Voltolina, S.; Gross, S. Dependence of calibration sensitivity of a polysulfone/Ru (II)-Tris (4, 7-diphenyl-1, 10-phenanthroline)-based oxygen optical sensor on its structural parameters. *Analytica chimica acta* **2008**, *627*, 239-246.

[11] Dordevic, N.; Beckwith, J.S.; Yarema, M.; Yarema, O.; Rosspeintner, A.; Yazdani, N.; Leuthold, J.; Vauthey, E.; Wood, V. Machine Learning for Analysis of Time-resolved Luminescence Data. *ACS Photonics* **2018**, *5*, 4888-4895.

[12] Chu, C.S.; Lin, K.Z.; Tang, Y.H. A new optical sensor for sensing oxygen based on phase shift detection. *Sensors and Actuators B: Chemical* **2016**, *223*, 606-612.

[13] Carraway, E. R.; Demas, J. N.; DeGraff B. A.; Bacon, J. R. Photophysics and Photochemistry of Oxygen Sensors Based on Luminescent Transition-Metal Complexes *Anal. Chem.* **1991**, *63*, 337342.

[14] Lippitsch, M.E.; Draxler, S. Luminescence decay-time-based optical sensors: principles and problems. *Sensors and Actuators B: Chemical* **1993**, *11*, 97-101.

[15] Digris, A.V.; Novikov, E.G.; Apanasovich, V.V. A fast algorithm for multi-exponential analysis of time-resolved frequency-domain data. *Optics communications* **2005**, *252*, 29-38.

[16] Stehning, C.; Holst, G.A. Addressing multiple indicators on a single optical fiber-digital signal processing approach for temperature compensated oxygen sensing. *IEEE Sensors Journal* **2004**, *4*, 153-159.

[17] Ogurtsov, V.I.; Papkovsky, D.B. Application of frequency spectroscopy to fluorescence-based oxygen sensors. *Sensors and Actuators B* **2006**, *113*, 608-616.

[18] Michelucci, U., *Applied Deep Learning - A Case-Based Approach to Understanding Deep Neural Networks*; Apress Media, LLC: New York, NY, USA, 2018; ISBN 978-1-4842-3789-2.

[19] Michelucci, U.; Baumgartner, M.; Venturini, F. Optical oxygen sensing with artificial intelligence. *Preprints* **2019**, 2019010047.

[20] Jones E, Oliphant E, Peterson P, et al. SciPy: Open Source Scientific Tools for Python. Available online: http://www.scipy.org/ (accessed on 26 December 2018).